

See discussions, stats, and author profiles for this publication at: <https://www.researchgate.net/publication/258115158>

# Interactive Forces between SDS-Suspended Single-Wall Carbon Nanotubes and Agarose Gels.

ARTICLE in JOURNAL OF THE AMERICAN CHEMICAL SOCIETY · OCTOBER 2013

Impact Factor: 12.11 · DOI: 10.1021/ja4052526 · Source: PubMed

CITATIONS

8

READS

72

5 AUTHORS, INCLUDING:



Justin G Clar

U.S. Environmental Protection Agency

6 PUBLICATIONS 10 CITATIONS

SEE PROFILE



Jean-Claude J Bonzongo

University of Florida

71 PUBLICATIONS 1,751 CITATIONS

SEE PROFILE



Kirk J Ziegler

University of Florida

78 PUBLICATIONS 2,178 CITATIONS

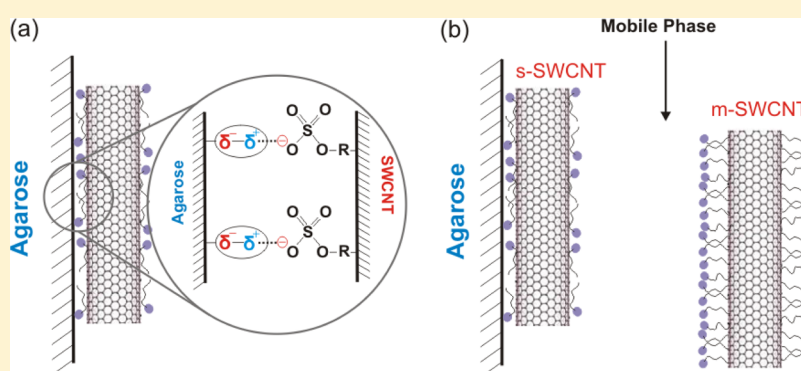
SEE PROFILE

## Interactive Forces between Sodium Dodecyl Sulfate-Suspended Single-Walled Carbon Nanotubes and Agarose Gels

Justin G. Clar,<sup>†</sup> Carlos A. Silvera Batista,<sup>‡,§</sup> Sejin Youn,<sup>†,||</sup> Jean-Claude J. Bonzongo,<sup>†</sup> and Kirk J. Ziegler<sup>\*,‡</sup>

<sup>†</sup>Department of Environmental Engineering Sciences and <sup>‡</sup>Department of Chemical Engineering, University of Florida, Gainesville, Florida 32611, United States

**S** Supporting Information



**ABSTRACT:** Selective adsorption onto agarose gels has become a powerful method to separate single-walled carbon nanotubes (SWCNTs). A better understanding of the nature of the interactive forces and specific sites responsible for adsorption should lead to significant improvements in the selectivity and yield of these separations. A combination of nonequilibrium and equilibrium studies are conducted to explore the potential role that van der Waals, ionic, hydrophobic,  $\pi$ - $\pi$ , and ion-dipole interactions have on the selective adsorption between agarose and SWCNTs suspended with sodium dodecyl sulfate (SDS). The results demonstrate that any modification to the agarose gel surface and, consequently, the permanent dipole moments of agarose drastically reduces the retention of SWCNTs. Because these permanent dipoles are critical to retention and the fact that SDS-SWCNTs function as macro-ions, it is proposed that ion-dipole forces are the primary interaction responsible for adsorption. The selectivity of adsorption may be attributed to variations in polarizability between nanotube types, which create differences in both the structure and mobility of surfactant. These differences affect the enthalpy and entropy of adsorption, and both play an integral part in the selectivity of adsorption. The overall adsorption process shows a complex behavior that is not well represented by the Langmuir model; therefore, calorimetric data should be used to extract thermodynamic information.

## INTRODUCTION

Since the discovery of single-walled carbon nanotubes (SWCNTs), researchers have envisioned many applications that take advantage of their astounding physical properties.<sup>1</sup> Conceptually, SWCNTs are a single-atom-thick sheet of graphene that is rolled into a seamless cylinder. The angle of this roll is defined by the unit vectors ( $n$ ,  $m$ ), which gives rise to SWCNTs with specific properties governed by the crystalline structure. When the difference between the values of  $n$  and  $m$  are divisible by 3, the SWCNTs are metallic (m); otherwise, the SWCNTs are semiconducting (s) with a defined band gap.<sup>2</sup> Theoretically, m-SWCNTs should make up a third of all possible nanotubes. Currently, all SWCNT synthetic approaches produce a variety of SWCNT ( $n$ ,  $m$ ) types that limit their use in many applications.<sup>3</sup> Although considerable progress has been made in controlling the diameters and types of SWCNTs produced,<sup>4,5</sup> a variety of postsynthesis separations are still required to produce nanotubes of specific length, diameter, and electronic type (i.e., purely m- or s-SWCNTs).<sup>6,7</sup>

Of particular interest over the last several years has been the development of a simple and scalable technique for the separation of SWCNTs. Several methods have been used to separate SWCNTs by chirality or by electronic type, including density gradient ultracentrifugation,<sup>8,9</sup> gel electrophoresis,<sup>10,11</sup> selective oxidation,<sup>12,13</sup> and selective wrapping with DNA,<sup>14,15</sup> polymers,<sup>16–18</sup> and amines.<sup>19,20</sup> While each of these techniques are capable of separating the m- and s-SWCNTs with varying levels of success, selective adsorption on agarose or dextran gels, which was pioneered by Kataura and co-workers,<sup>21,22</sup> is currently one of the most promising methods for large-scale, high-throughput separations.

While the use of agarose gel columns has been effective in separating m- and s-SWCNTs, little is understood about the mechanism. Our prior study<sup>23</sup> proposed that the mechanism was due to selective retention of s-SWCNTs, which was later

Received: May 24, 2013

Table 1. Characteristics of Gel Media Used in This Work

medium	type <sup>a</sup>	group	ligand density ( $\mu\text{mol/mL}$ )	pore size (nm)	% agarose
Sepharose 6 FF	SEC			29 <sup>c</sup>	6
Sepharose 4 FF	SEC			45 <sup>c</sup>	4
sp-Sepharose 6 FF	IEX	(−) sulfopropyl	<i>b</i>	24 <sup>d</sup>	6
Q-Sepharose 6 FF	IEX	(+) quaternary ammonium	<i>b</i>	29 <sup>e</sup>	6
phenyl-Sepharose (HS)	HIC	phenyl	40		6
phenyl-Sepharose (LS)	HIC	phenyl	25	35 <sup>f</sup>	6
butyl-Sepharose	HIC	butyl	40		4
octyl-Sepharose	HIC	octyl	5		4

<sup>a</sup>Typical purpose of the gel medium: size-exclusion (SEC), hydrophobic interaction (HIC), or ion-exchange (IEX) chromatography. <sup>b</sup>Ligand density for charged groups depends on the eluent and is difficult to characterize. <sup>c</sup>Hagel et al. <sup>27</sup> <sup>d</sup>DePhillips and Lenhoff. <sup>28</sup> <sup>e</sup>Yao and Lenhoff. <sup>29</sup> <sup>f</sup>Evans et al. <sup>30</sup>

confirmed by the work of Tvrdy et al.<sup>24</sup> As highlighted in our previous study, the selective adsorption was controlled by the packing of sodium dodecyl sulfate (SDS) molecules around SWCNTs.<sup>23</sup> This mechanism implies inherent differences in surfactant structure around m- and s-SWCNTs in the suspension. Indeed, other researchers have observed different buoyancies for m- and s-SWCNTs,<sup>9</sup> which suggests differences in surfactant coverage for each SWCNT type. Molecular dynamics simulations have also shown that different surfactant structures are formed around specific (*n*, *m*) types.<sup>25,26</sup> In this paper, we aim to understand the nature of intermolecular forces that yield selective adsorption of SDS–SWCNTs onto agarose gel. The heterogeneous interface of the SDS–SWCNT complexes (i.e., the coexistence of hydrophobic and hydrophilic patches), the dynamic nature of SDS molecules on SWCNTs, and the complex micro- and macrostructure of agarose gels allows for a variety of potential interactive forces (e.g., ionic, van der Waals, hydrophobic). In order to probe the nature of these interactions, the contribution from each of these forces are either inhibited or enhanced to determine their relative importance in the selective retention of s-SWCNTs onto agarose. By understanding the interaction of SWCNTs with the agarose gel under both equilibrium and non-equilibrium conditions, we aim to identify the primary force responsible for selective adsorption. Furthermore, we discuss possible reasons why SDS–SWCNTs show a larger affinity for agarose gels than SWCNTs coated with other surfactants, such as sodium cholate (SC), as well as a description of the active adsorption sites within the agarose gels. This knowledge should lead to more efficient separations of SWCNTs.

## METHODS

**Materials.** Nanopure water was used in all experiments. SDS (>99%) and SC (>99%) were purchased from Sigma–Aldrich (St. Louis, MO) and used as received. HiPco SWCNTs were obtained from Rice University (Rice HPR 162.3) and used as received. Different stationary phases were used as the adsorbent, including plain agarose (Sepharose 6 and 4 FF) and agarose functionalized with either hydrophobic aliphatic carbon chains (butyl- and octyl-Sepharose 4 FF), hydrophobic phenyl groups (phenyl-Sepharose 6 FF) at both low and high substitution (LS and HS, respectively), or ionic groups (sp- and Q-Sepharose 6 FF). All the gels were manufactured by GE. Phenyl-Sepharose HS was purchased from Sigma–Aldrich, whereas the other gels were obtained from GE Health Care. The average diameter of all the gel beads was 95  $\mu\text{m}$ . Table 1 summarizes the relevant properties of the gel media used as the stationary phase. It is important to note that Sepharose 4 and 6 FF are highly cross-linked in comparison to the Sepharose 6B used in many studies, providing a more rigid structure.

**Aqueous SWCNT Suspensions.** Aqueous suspensions of SWCNTs were prepared as described in our previous work.<sup>23</sup> Briefly,

30–40 mg of raw SWCNTs was added to 100 mL of a 1 wt % SDS solution in Nanopure water. The solution was then homogenized for 30 min (IKA T-25 Ultra-Turrax) and ultrasonicated (Misonix S3000) for 10 min (120 W) to aid dispersion. After ultrasonication, the resulting mixture was ultracentrifuged (Beckman Coulter Optima L-80 K, SW 28 rotor) at 20 000 rpm (53 000g). Ultracentrifugation times varied for nonequilibrium (4 h) and equilibrium experiments (1 h) to produce the desired concentration of SWCNTs. A comparison of the absorbance and fluorescence spectra for both SWCNT suspensions is shown in Figure S1 (Supporting Information). Although there is some broadening in the absorption spectra of SWCNTs used in the equilibrium studies, both suspensions give intense fluorescence, suggesting a high-quality dispersion.

**Equilibrium Adsorption.** The agarose gels were thoroughly rinsed with Nanopure water to remove any residual ethanol used as a preservative prior to their use. The rinsed gels were then equilibrated with a 1 wt % SDS solution (SDS solution/gel volume ratio of 2:1). Approximately 500  $\mu\text{L}$  of surfactant-stabilized gel was used for each replicate in separate 15 mL centrifuge tubes. Individual replicates were equilibrated with various concentrations of SWCNT in a constant background solution of 1 wt % SDS. After all components were combined, the samples were mixed in a vortex stirrer for 30 s before being placed in a water bath held at 25  $^{\circ}\text{C}$  for 24 h to ensure equilibration. After stabilization, samples were centrifuged for 5 min at 5000 rpm to remove any agarose beads from the supernatant. An aliquot of the supernatant (300  $\mu\text{L}$ ) was then extracted and analyzed by absorption and fluorescence spectroscopy, as described below.

**Nonequilibrium Adsorption.** Columns were packed with different compositions of agarose beads up to 6 cm in height. The columns were first stabilized with at least five column volumes (CV), approximately 43 mL, of 1 wt % SDS solution. For the experiments with the IEX media, equilibration required more volume; these columns were stabilized with 16 CV. Half a column volume of the suspension was then injected into the column. The early fractions of SWCNTs were eluted with 1 CV of 1 wt % SDS solution followed by two CV of 2 wt % SC solution to remove the retained SWCNTs from the column. Each fraction was then characterized by absorption and fluorescence spectroscopy, as described below.

**SWCNT Characterization.** The initial SWCNT suspensions and the supernatant extracted from the equilibrium studies were characterized by absorption (0.4 cm path) and fluorescence (1 cm path) spectroscopy on an Applied NanoFluorescence Nanospectra-lyzer (Houston, TX) with excitation from 662 and 784 nm diode lasers. Effluent from the column was continuously characterized in situ by use of a flow cell from Starna Cells as previously described.<sup>23</sup> Typically, absorption spectra were taken every 20 s as the effluent flowed through the cell. Mass fractions of SWCNTs eluted during separation were estimated by use of absorbance values at 626 nm, where the extinction coefficient was calculated on the basis of the one determined by Moore et al.<sup>31</sup> at 763 nm (see Supporting Information).

The distribution of SWCNT lengths was measured by atomic force microscopy (AFM) following the procedure published by Khripin et al.<sup>32</sup> Silicon wafers were functionalized with 3-(ethoxydimethylsilyl)-propylamine (APDMES, Sigma–Aldrich, St. Louis, MO). Before 157

deposition on the substrate, SWCNT samples in 1 wt % SDS were diluted at least 100X with an aqueous solution of 0.2 wt % SC and 20 mM NaSCN. SWCNTs were deposited on the wafer by casting 10  $\mu$ L of the sample, followed by incubation in a closed container for 6 min. After incubation, samples were dried by use of canned nitrogen. Several images were acquired on a Bruker Dimension Icon AFM in the peak-force tapping mode (ScanAsyst) with the respective ScanAsyst-Air probes. By this method, the average SWCNT length was calculated to be 467 nm. A representative AFM image and length distribution histogram are shown in Figure S2 (Supporting Information).

## RESULTS AND DISCUSSION

**Physical and Chemical Structure of Agarose Gels.** The agarose polymer is the major gelling constituent of agar and contains agarobiose as the monomeric unit,<sup>33</sup> as Figure 1a shows. The porous 3D structure of agarose is due to the self-assembly of molecules at the nano- and microscale.<sup>33</sup> At the nanoscale, single strands of agarose form double helices that are stabilized by intra- and intermolecular hydrogen bonds. Further aggregation of individual helices into bundles of various size

and structure result in the characteristic porous 3D nature of agarose (see Figure 1b). The porous structure of the resulting beads is dependent upon the concentration of agarose used during production. The pore size decreases slightly as the concentration of agarose used in production increases from 4% to 6%. For example, the average pore size for Sepharose 4 and 6 FF is 45 and 29 nm, respectively.<sup>27</sup> Furthermore, electric birefringence studies have reported large, permanent dipoles in the range  $10^3$ – $10^6$  D for agarose.<sup>35–38</sup> Importantly, these studies showed that domains of different size within agarose align at various time scales when placed in an electric field, suggesting different dipole moments. This observation indicates that agarose gels are formed by the nonuniform and random network shown in Figure 1b. Finally, the size of the domains aligned by the applied electric field and, consequently, the dipole moments changed as the concentration of agarose was altered.

Initially, the attractiveness of agarose as a size-exclusion (SEC) medium in biochemistry stemmed from its hydrophilicity (large number of ether and hydroxide groups), its stability in a wide range of pH values, and concomitant neutrality that minimizes the nonspecific binding of proteins. However, residual charges on the surface as well as hydrophobic groups from the manufacturing process can potentially exist, promoting protein binding to the gel according to their hydrophobic character or their charge density.<sup>39,40</sup> Consequently, residual contaminant moieties could influence the adsorption of SDS–SWCNTs despite pure agarose being neutral and hydrophilic.

Although agarose can potentially have small regions of hydrophobic and ionic groups that offer selective adsorption, the surface can be additionally functionalized with either hydrophobic or ionic groups to further promote these interactions and aid separation. The glycidyl ether chemistry couples the ligand group to the agarose matrix by reacting with the hydroxyl groups on the backbone, resulting in the structures depicted in Figure 1c.<sup>41</sup> It is critical to note that any functionalization to the base agarose matrix (i.e., phenyl, octyl, etc.) will not significantly alter the average pore size (see Table 1). However, functionalization of the agarose base may alter the magnitude of the permanent dipole moments, which could affect separation.

**Retention of SDS–SWCNTs on Agarose Gels.** The affinity of agarose toward SDS–SWCNTs has already been exploited for the separation of nanotubes.<sup>10,21,22,42,43</sup> Figure 2a shows the elution curves of SDS–SWCNTs as they pass through a column packed with one of the base materials (Sepharose 6 FF). Similar to prior experiments with Sepharose 6B, a large percentage of SWCNTs are adsorbed onto the agarose beads. The fraction of nanotubes that pass through the column (peak P1) is highly enriched in m-SWCNTs, as shown by the absorbance spectra in Figure 2b, while the nanotubes eluted with 2% SC (peak P2) are primarily s-SWCNTs. In general, all the unfunctionalized agarose beads (4 FF, 6 FF, and 6B) are capable of separating SWCNTs. The most appreciable difference observed among the different variants of agarose is in the shape of adsorption isotherms (see Figure S3 in Supporting Information). The difference in adsorption isotherm shape behavior between Sepharose 6 FF and 4 FF confirms an inverse relationship between the concentration of agarose in the gel matrix and SDS–SWCNT retention.<sup>44</sup> This may seem counterintuitive at first, but a possible explanation lies in the

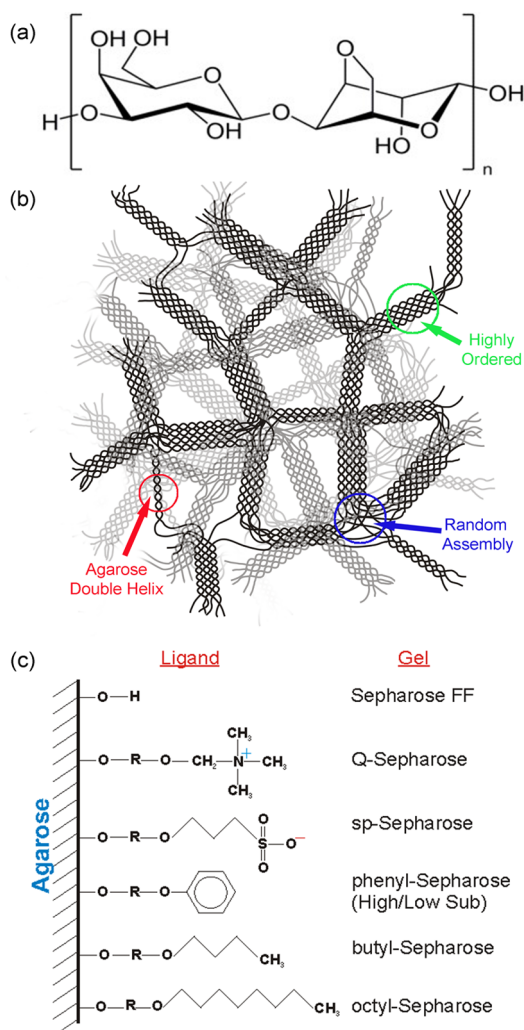


**Figure 1.** Physical and chemical structure of agarose. (a) Monomeric unit of agarose chains. (b) Polymers organize into double helices and are further stabilized by bundling to form aggregates of various structure and size. Adapted image from Arnott et al.<sup>34</sup> (c) Ligands added to agarose backbone after functionalization. The R group represents  $\text{CH}_2\text{CH}(\text{OH})\text{CH}_2$  chains added through a glycidyl ether coupling reaction.



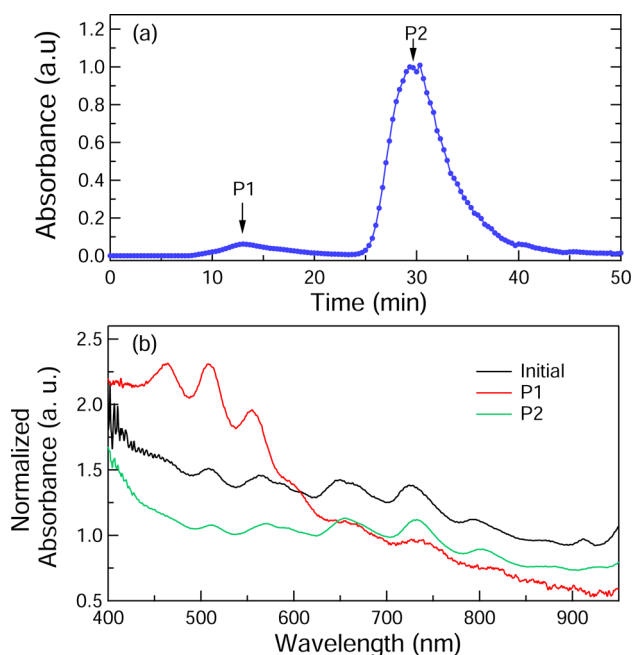


**Figure 2.** (a) Elution curve of SWCNTs suspended in 1 wt % SDS with Sepharose 6 FF as the stationary phase. The SWCNT suspension is injected at time 0. The elution curve is presented in terms of absorbance of effluent normalized by absorbance of initial suspension ( $\lambda = 626$  nm). (b) Absorbance spectra from initial sample and effluent at the first (P1) and second (P2) peaks of the elution curve. Spectra of P1 and P2 have been slightly offset for visual clarity.

synthesis. More importantly, these OH groups are also highly polarizable, and it is reasonable that the permanent dipoles observed in electric birefringence measurements<sup>35–38</sup> are associated with these groups. The existence of these dipole regions creates the potential for an attractive interaction with an approaching charge.

The interface of SDS–SWCNTs is equally intricate. The structure of the surfactant shell around nanotubes is dynamic, not well-defined, and is expected to be heterogeneous, with some areas of the SWCNT completely exposed to the medium. Hence, the SWCNT interface might present distinct hydrophobic and hydrophilic regions that provide the possibility of different interactions with agarose. Simulation studies have shown that the structure of the surfactant shell depends on concentration,<sup>25,26</sup> while buoyancy differences suggest structural variability in surfactant coverage based on the metallic or semiconducting nature of the SWCNTs<sup>9,46</sup>. Finally, SDS molecules bound to the SWCNTs are highly mobile, as demonstrated by the ability of SDS molecules to change their assembly under different mechanical and chemical stimuli, such as shearing,<sup>47</sup> uptake of nonpolar compounds,<sup>23,48</sup> or changes in the ionic strength of the medium.<sup>9,23,46</sup>

Given the physical and chemical structure of agarose as well as the complicated interface of surfactant-suspended SWCNTs, both long- and short-range interactions are possible. However, only a finite number of interactions can exist between the agarose and SWCNTs once their structures are considered. The hydrophobic regions of both the agarose and SWCNTs may yield weak, short-range forces important to the separation, such as van der Waals (vdW), hydrophobic, and  $\pi$ – $\pi$  interactions. On the other hand, the hydrophilic groups on each enable strong, long-range forces, such as ionic or ion–dipole interactions. While multiple interactions may be occurring between SWCNTs and agarose, the relative importance of a given force can be evaluated by either inhibiting or promoting its significance during adsorption. We begin by investigating the role of vdW forces by inhibiting ionic interactions. Next, ionic, hydrophobic, and  $\pi$ – $\pi$  interactions are promoted by systematically modifying the surface of the stationary phase with aliphatic, phenyl, and charged groups, as shown in Figure 1c.

**Adsorption Predominantly through van der Waals Interactions.** While vdW forces are generally weaker than ionic interactions, they are additive along the length of the nanotube in these systems and can provide significant adsorption onto a surface. Furthermore, recent studies using Lifshitz theory quantified the differences in vdW forces between SWCNTs of different type and chirality.<sup>49,50</sup> These theoretical studies reported significant differences in vdW potentials between m- and s-SWCNTs,<sup>49</sup> as well as increased attraction of s-SWCNTs over m-SWCNTs toward polymer surfaces.<sup>50</sup> Although the agarose gels used here have considerable differences from the polymers in those studies, vdW interactions could be a driving force during the gel-based separation of SDS–SWCNTs.

To investigate the relative importance of vdW interactions during separation, equilibrium studies were conducted with Sepharose 4 and 6 FF. Each gel was equilibrated with identical concentrations of SDS-suspended SWCNTs with an increasing electrolyte background up to 80 mM NaCl. Increasing the ionic strength of the solution has several important effects. Most importantly, the increase in charge screening drastically compresses the size of the electric double layer. This compression serves to minimize the range and intensity of

different structures (see Figure 1b) formed during synthesis, as supported by electric birefringence studies.<sup>35–38</sup>

When one attempts to understand the fundamental mechanisms responsible for the separation of nanotubes via agarose gels, the physical parameters of SWCNTs and agarose must be considered. If one considers the average pore size of the base agarose (45 nm or less) as well as the average length of the SWCNTs used in this study (>100 nm as shown in Figure S2, Supporting Information), it is unlikely that a significant amount of SWCNTs diffuse into the pores of the agarose gel. Given that the bead size is the same for all agarose used in this study and that the hydrophobicity of a surface does not significantly affect the slip plane,<sup>45</sup> no hydrodynamic effects should be responsible for changes in retention either. As the pore size of the beads is primarily determined by the percentage of agarose used during production, any functionalization of the backbone does not significantly alter the pore size (see Table 1). The agarose gels are equilibrated with significant amounts of SDS (5 CV) prior to separation, so any interaction between the surfactant and functional groups cannot alter the dispersion properties of SWCNTs. Therefore, modification to agarose should affect only the interaction of SWCNTs with the outer surface of the agarose beads. The fact that SDS–SWCNT separations are effective with both the beaded and nonbeaded gel forms of agarose supports the assertion that the selective retention of s-SWCNT must be governed by surface interaction and not transport through pores.

**Probing the Interaction of SWCNTs with Agarose.** As described above, the structure of agarose used for these column-based separations is complex. The hydrophilic regions are represented by the ubiquitous hydroxyl groups (each monomer contains four OH groups) depicted in Figure 1a, while the potential hydrophobic regions include residues from

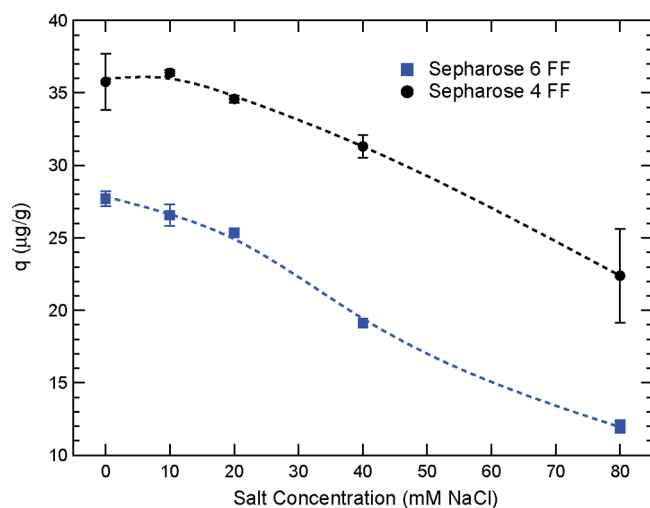


**Figure 3.** Comparison of retention behavior of 1 wt % SDS-SWCNT suspension in plain Sepharose 4 FF and 6 FF at different electrolyte concentrations.

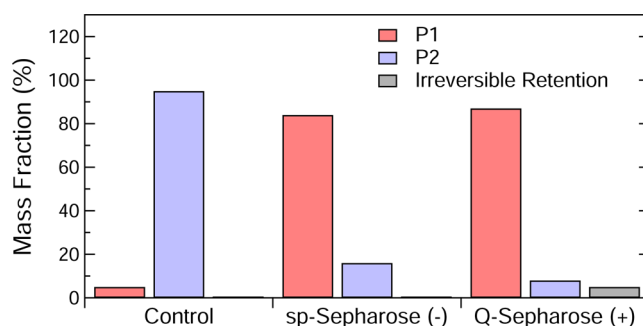


**Figure 4.** Retention behavior of 1 wt % SDS-SWCNT suspension in plain Sepharose 6 FF and Sepharose 6 FF functionalized with ionic groups, sp- and Q-, that contain negative and positive charges, respectively. Bars indicate the mass fraction of SWCNTs eluted in peaks 1 (P1) and 2 (P2) as well as those that are irreversibly retained (not eluted with 2 wt % SC) within the column. All three columns were stabilized with 16 CV of 1 wt % SDS buffer prior to SWCNT injection.

Sepharose is negatively charged, 15% of SDS-SWCNTs are still adsorbed, suggesting that there are adsorption sites strong enough to compete with the repulsion from the negative groups. Interestingly, Q-Sepharose also has little retention of SWCNTs despite bearing positive surface charges. It is important to note that the common procedure for all column separations is to equilibrate the surface with the surfactant prior to SWCNT injection. Any positive charges that exist on the agarose (backbone or functional groups) would then be covered with SDS during equilibration. Therefore, the lack of adsorption simply shows that SDS is not extensively displaced by SDS-coated SWCNTs. We do note that a small portion of the SWCNTs are irreversibly retained, suggesting that some SWCNTs are able to strongly adsorb onto the surface. In general, there is no driving force for SDS-SWCNTs to displace SDS molecules from the surface. If either charge were responsible for the retention of SDS-SWCNTs, increasing the number density of that charge would have increased the amount of SWCNTs adsorbed. Since a reduction in retention was observed, electrostatic attraction (ion exchange) is not the dominant interaction between SDS-SWCNT complexes and agarose.

**Adsorption Predominantly through Hydrophobic Interactions.** The importance of hydrophobic interactions was tested by using a set of Sepharose beads that have been functionalized with butyl and octyl groups. Figure 5 compares the retention and adsorption behavior of plain, butyl-, and octyl-Sepharose under equilibrium and nonequilibrium conditions. Once the Sepharose is functionalized with aliphatic groups, both nonequilibrium and equilibrium adsorption studies show that retention of SDS-SWCNTs decreases substantially. During column experiments with butyl-Sepharose, only 27% of the injected SWCNTs are retained on the column. This low adsorption affinity is confirmed by the limited retention (16 μg/g) shown in equilibrium experiments. Decreased retention is also evident in the octyl-Sepharose systems (65% and 45 μg/g). The resulting absorbance spectra from nonequilibrium studies (see Figure S5 in Supporting Information) also demonstrate a nearly complete loss of selectivity once Sepharose 4 FF is functionalized. Finally, it is important to note that functionalization of the base gel creates drastic changes to the shape of the adsorption isotherms presented in Figure 5. For example, the multiple plateaus at 18

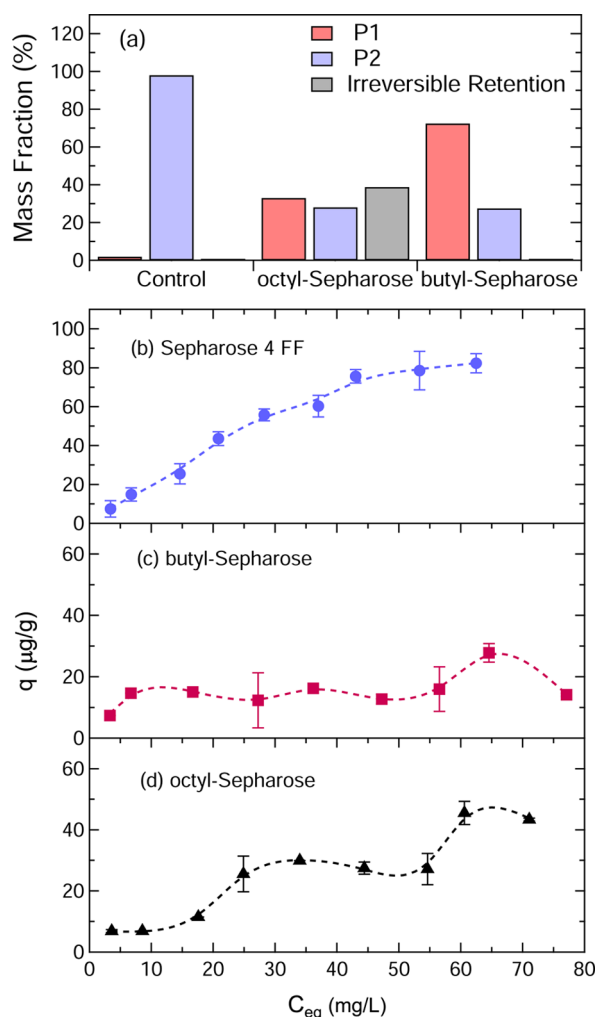


**Figure 5.** Retention behavior of 1 wt % SDS–SWCNT suspension in plain Sepharose 4 FF and Sepharose 4 FF functionalized with octyl and butyl groups. (a) Comparison of the mass fraction of SWCNTs eluted in peaks 1 (P1) and 2 (P2) as well as those that are irreversibly retained within the column during nonequilibrium studies. (b–d) Equilibrium adsorption isotherms for (b) plain Sepharose 4 FF (●), (c) butyl-Sepharose (■), and (d) octyl-Sepharose (▲). Note that the equilibrium concentration ( $C_{eq}$ ) is given in milligrams per liter, while the amount of adsorbed SWCNTs ( $q$ ) is given in micrograms per gram.

degrees of phenyl substitution (see Table 1) were used to observe the changes in adsorption behavior as the concentration of phenyl groups on Sepharose 6 FF was changed from 0 to 40  $\mu\text{mol/mL}$ . Figure 6 shows the retention characteristics

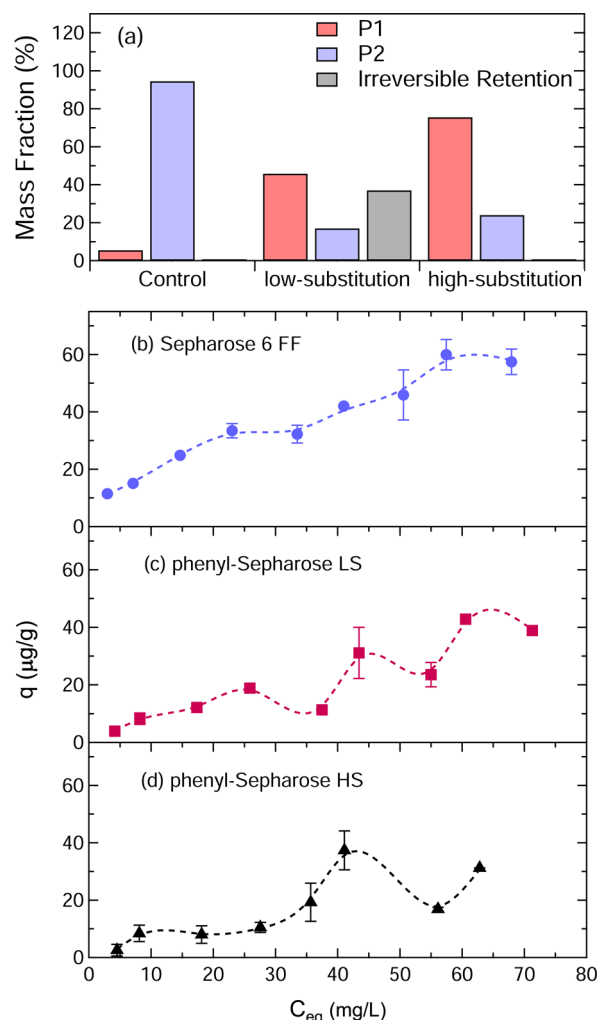


**Figure 6.** Retention behavior of 1 wt % SDS–SWCNT suspension in plain Sepharose 6 FF and Sepharose 6 FF functionalized with phenyl groups at low and high substitution. (a) Comparison of the mass fraction of SWCNTs eluted in peaks 1 (P1) and 2 (P2) as well as those that are irreversibly retained within the column during nonequilibrium studies. (b–d) Equilibrium adsorption isotherms for (b) plain Sepharose 6 FF (●) and phenyl-Sepharose at (c) low (■) and (d) high substitution (▲).

of SDS–SWCNTs on phenyl-Sepharose. Similar to the studies of hydrophobic interactions, both nonequilibrium and equilibrium studies of phenyl-substituted agarose showed decreases in retention. These decreases in retention, however, were dependent on the surface concentration of the functional groups. At low substitution, phenyl-Sepharose retained 54% of SDS–SWCNTs, whereas it retained only 25% at high substitution (see Figure 6a). This reduction in retention by almost half occurs while the ligand density is nearly doubled from 25 to 40  $\mu\text{mol/L}$ . Once the matrix is functionalized with phenyl-Sepharose at either degree of substitution, the adsorption isotherms change dramatically (see Figure 6b–d). The slope of the isotherms is shallow in comparison with that of Sepharose 6 FF, showing decreased affinity for the surface.



These isotherms also show unique nonmonotonic shapes not seen in the unfunctionalized agarose beads, which will be discussed later. Similar to the studies of agarose functionalized with aliphatic groups, the absorbance spectra show that any retention that is occurring is not selective (see Figure S6 in Supporting Information).

The results from both equilibrium and nonequilibrium studies are similar regarding the potential of  $\pi$ - $\pi$  interaction to drive the separation of SWCNTs in these systems. A systematic increase to the density of phenyl groups on the surface of the gel did not increase SDS-SWCNT retention in either system. Therefore,  $\pi$ - $\pi$  interactions between SDS-SWCNTs and agarose are not the primary driving force for selective adsorption of SDS-SWCNTs.

#### Nature of Adsorption between SWCNTs and Agarose.

##### Role of Ion-Dipole Interactions in Selective Adsorption.

Direct measurement of the extent of ion-dipole interactions between SDS-SWCNTs and agarose gels is difficult for several reasons. By their very nature, ion-dipole interactions are mixed systems; therefore, suppressing other forces without affecting ion-dipole interactions is unlikely. Enhancing their interaction by directly manipulating the charge density of ions (SDS-SWCNTs) or dipoles (agarose) is also not feasible. SDS-SWCNTs are already coated with a substantial amount of anionic charges and essentially act as macro-ions. As a result, an attempt to increase the charge density of SDS on SWCNTs will likely alter the structure of the surfactant on the sidewalls, indirectly affecting the interaction with agarose. Likewise, the permanent dipole moments of agarose<sup>35-38</sup> most likely originate from the ubiquitous placement of highly polarizable OH groups. Increasing the concentration of OH groups beyond the base material is unlikely.

While there is inherent difficulty in directly measuring ion-dipole interactions, these forces remain a strong candidate for adsorption due to SDS-SWCNTs acting essentially as macro-ions and the presence of permanent dipoles in the agarose matrix.<sup>35-38</sup> It is critical to note that the charged head groups of SDS used to stabilize the nanotubes must play a crucial role in the separation of SWCNT suspensions. The results presented in Figure 3 show that screening the charges on SDS results in reduced SWCNT retention. Previous studies have also shown little to no separation when one attempts to separate SWCNT dispersed in other surfactants or with concentrations of SDS lower than 0.5 wt %.<sup>22,43</sup> Therefore, any force responsible for retention of SDS-SWCNT during separation must account for the fact that the electric potential (charged surface) of SDS-SWCNTs is essential for retention on neutral agarose. Interestingly, ion-dipole interactions account for this observation. Furthermore, if ionic, hydrophobic, or  $\pi$ - $\pi$  interactions were dominant in the selective adsorption of SWCNTs, increasing their density should have yielded higher retention of SWCNTs. Figure 7 shows that any modification to the agarose base significantly decreases the retention of s-SWCNTs, especially in nonequilibrium systems. In fact, a strong inverse relationship is observed with ligand density regardless of the functional group. In nonequilibrium conditions, butyl- and phenyl-Sepharose HS, which both have a ligand density of 40  $\mu\text{mol/mL}$ , retain a similar amount of SWCNTs despite the ligand groups being different. Changes to the highly polarizable OH groups during functionalization will likely alter the overall dipole moment of the matrix, which would reduce retention if ion-dipole interactions were important. As the ligand density increases, more OH groups

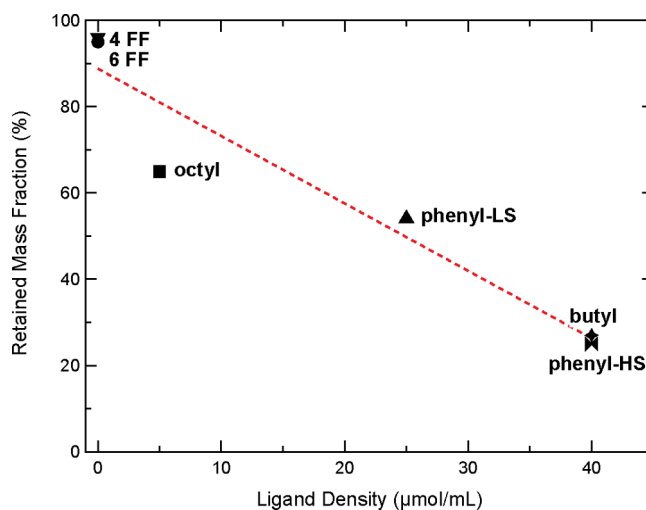


**Figure 7.** Relationship between ligand density and the mass of SDS-SWCNTs retained by different gel media in nonequilibrium (column) studies.

are altered on agarose, enhancing this effect. The ligand density also affects the selectivity of the matrix. The retention by matrices functionalized with ligand densities higher than 5  $\mu\text{mol/mL}$  is not selective (see Figures S4-S6 in Supporting Information). The only functionalized matrix that shows a slight degree of selective retention is octyl-Sepharose, which also has the lowest degree of substitution (5  $\mu\text{mol/mL}$ ). Therefore, the presence of permanent dipoles appears to be important to retention and selectivity.

The results indicate that both the ionic charge on nanotubes and the permanent dipole on agarose gels are important to both retention and selectivity. Therefore, it is logical that ion-dipole interactions play a dominant role in the selective adsorption of SWCNTs, as shown in Figure 8a. In some sense, this type of interaction with agarose is similar to those that take place between agarose and other solutes in what is called hydrophilic interaction chromatography.<sup>53</sup>

**Role of SDS in Separation Selectivity.** While ion-dipole interactions can account for the adsorption of SDS-SWCNTs on agarose gel, questions still remain regarding the nature of selectivity, whereby s-SWCNTs are initially retained by the gel and m-SWCNTs are eluted. As ion-dipole interactions carry no inherent selectivity on their own, the separation must be driven by inherent differences between the s- and m-SWCNT species. We propose that the origin of selective adsorption is due to differences in polarizability of SWCNT species. Previous studies have suggested that a charge (i.e., SDS headgroups) in proximity to a polarizable object, such as a SWCNT, can induce image charges on the SWCNT.<sup>9,54,58</sup> The induced image charges on the SWCNTs serve to screen the SDS headgroups from one another, as well as screening the SWCNTs from other approaching charges (i.e., permanent dipoles on agarose), thereby lowering their overall potential. Both theoretical calculations<sup>55</sup> and laboratory AFM measurements<sup>56</sup> have demonstrated large differences in polarizability of m- and s-SWCNT types, whereby the polarizability of m-SWCNTs was 3 orders of magnitude higher than their s-SWCNT counterparts. The magnitude of the image charges formed is dependent upon the polarizability of the object; therefore, image charges are more easily induced on m-SWCNTs, allowing SDS molecules to pack more tightly around m-SWCNTs.<sup>9,46</sup> As a result, the



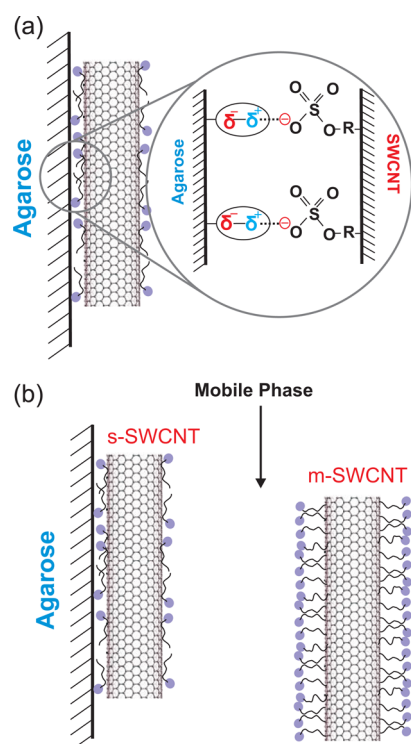


**Figure 8.** Mechanism of interaction and selectivity during agarose gel-based separations of SDS–SWCNTs. (a) Dipoles on the agarose gel surface enable interaction with negatively charged head groups of SDS on SWCNTs. (b) Higher polarizability or differences in vdW forces alter the surfactant structure around m-SWCNTs, thereby minimizing the interaction potential between m-SWCNTs and agarose gels.

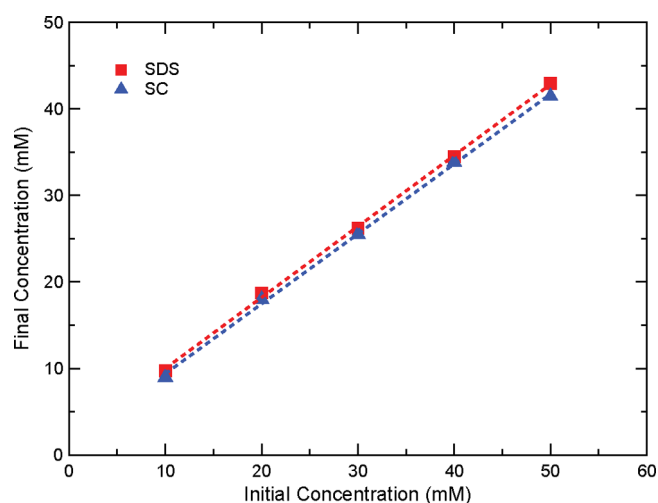


**Figure 9.** Retention of surfactants used in agarose gel separations on Sepharose 6 FF. The figure shows the final (■) SDS and (▲) SC surfactant concentration that remains in the supernatant after equilibrium. Final concentrations were determined by densitometry.

SWCNT adsorption must be due to the SWCNT–surfactant complex.

Clearly there must be differences in SDS– and SC–SWCNT suspensions that promote their variant interactions with agarose. A possible explanation can be obtained by looking at the differences in the shell of both surfactants and its effect on the hydrogen bonds and structure of water molecules. As we previously demonstrated, SDS molecules on SWCNTs are mobile and rearrange in response to chemical and mechanical stimuli.<sup>23,47,48,57</sup> Furthermore, simulation studies indicate that SDS molecules align with the axis of a SWCNT, exposing their hydrophobic tail considerably to the aqueous phase and leaving large areas of the nanotube surface bare.<sup>25,26</sup> In contrast, SC (or sodium deoxycholate) molecules are considered to be much more tightly bound to the surface and do not rearrange in response to chemical or mechanical stimuli, providing better coverage of the SWCNT surface. Moreover, SC molecules bind to the SWCNT surface with their hydrophobic face in contact with the nanotube surface, while their hydrophilic face is exposed to water. Whenever water molecules accommodate nonpolar and hydrophobic molecules, the water molecules in their vicinity are more structured, due to the loss of degrees of freedom and consequently entropy.<sup>58,59</sup> Hence, water should be more structured in the vicinity of SDS–SWCNTs than for SC–SWCNTs due to the interaction of water with the hydrophobic SDS tails and bare nanotube surface. The adsorption of SDS–SWCNTs to agarose will then lead to a net gain of entropy. Although the entropy decreases during adsorption from the reduced SDS degrees of freedom, that entropy loss can be compensated for and surpassed by a gain in entropy from the recovery of degrees of freedom of water. The process is analogous to micellization, where the formation of micelles results in a loss of degrees of freedom for surfactant molecules inside the micelles but a net gain in entropy due to the recovery of degrees of freedom of water. By the same reasoning, these entropic effects can explain why higher concentrations of SDS can desorb SWCNTs<sup>60,61</sup> and why the solubilization of organic molecules on the surfactant shell reduces the adsorption of SDS–SWCNTs.<sup>23</sup> Both higher concentrations of SDS<sup>25,26,46</sup> and the solubilization of organic molecules<sup>48,57</sup> change the assembly of SDS molecules on SWCNTs in such a way that the

interaction strength between m-SWCNTs and the dipoles on agarose are lower due to both the ion–dipole repulsion provided by the image charges and the steric repulsion provided by a higher aggregation number of surfactant, as described in our prior work.<sup>23</sup> The combination of these effects produces a much lower affinity of m-SWCNTs toward agarose than s-SWCNTs, as shown in Figure 8b. It is also plausible that the inherent differences in vdW forces for m- and s-SWCNTs calculated by Lifshitz theory<sup>49,50</sup> help drive the formation of unique surfactant structures surrounding each type of SWCNT (m- or s-). The differences in packing of surfactant on the SWCNT sidewalls would subsequently cause similar differences in image charge.

It is interesting to note that these effects should exist for all nanotubes suspended with ionic surfactants, meaning that agarose should be able to separate any SWCNTs suspended with anionic surfactants. However, selective adsorption is typically observed for only SDS–SWCNTs, whereas a SC–SWCNT suspension introduced into the column shows almost no retention. If the enthalpic effects described above could solely describe the adsorption of nanotubes, one would expect similar results for SDS– and SC–SWCNTs. It is possible that the surfactants themselves exhibit different interactions with the agarose that could explain the differences in adsorption for SDS– and SC–SWCNTs. However, Figure 9 shows that the SDS and SC molecules by themselves have almost no differences in their interaction with agarose, indicating that any energetic difference between the surfactant molecules is minimal. These results indicate that any differences seen in

hydrophobic tails of SDS molecules are hidden from the aqueous phase.

In summary, adsorption between SDS–SWCNTs and agarose occurs through an ion–dipole interaction. While the selective structures formed around m- and s-SWCNTs will have implications on the enthalpic interactions, the entropic differences also must have an important role in the selective retention of SDS–SWCNTs.

**Adsorption Isotherm Behavior.** Although others have assumed that the adsorption isotherms of SWCNTs on agarose gels are Langmuir-type, the isotherms in Figures 5 and 6 cannot be described adequately by a Langmuir isotherm. It is also particularly important to note that the error bars depicted in these figures are very small for most data sets. The error bars increase only at the step edge or transition region before a stable plateau, where slight concentration differences would yield large changes to retention. A Langmuir isotherm is represented by increasing adsorption until a plateau, or saturation point, is reached, which represents thermodynamic equilibrium and complete occupation of the adsorption sites. This theoretical Langmuir shape is driven by the assumption that the adsorbent contains a fixed number of adsorption sites of equal energy, resulting in monolayer coverage of the solid adsorbent, and that there is no interaction between the solutes. The non-Langmuir shape of all isotherms suggest that adsorption sites may have different locations/conformations producing various energy barriers to adsorption.<sup>62</sup> As functional groups are added to the agarose backbone, the differences between these energy sites becomes more clear. These differences could indicate that regions with distinct magnitudes of permanent dipole moments account for these discrete energy sites. For the octyl-Sepharose system presented in Figure 5 as an example, the multiple plateaus indicate either that SWCNTs deposit as multiple layers on the surface of octyl-Sepharose or that the number/energy of adsorption sites do not remain constant as the applied concentration of SWCNTs is increased. Interestingly, the adsorption isotherms for pure agarose (see Figures 5 and 6 and Figure S3 in Supporting Information) do not exhibit Langmuir behavior either, despite its persistent use in the literature.<sup>44,63,64</sup>

Adsorption of SWCNTs onto agarose appears to follow isotherms that do not assume homogeneity in the energy of adsorption sites (e.g., Freundlich) or the formation of a monolayer on the surface of the gel (e.g., Brunauer–Emmett–Teller).<sup>62,65</sup> Again, agarose contains multiple ordered structural domains, each with different dipole moments. By their nature, SDS–SWCNT suspensions are heterogeneous in length distribution (see Figure S2 in Supporting Information). Accordingly, the number of adsorption sites (total energy of adsorption) should be proportional to nanotube length. The dynamic nature of the SDS–SWCNT interface and the permanent dipoles of different magnitude within agarose suggest that binding events of different energies are probable. Furthermore, the number of different packing configurations of cylinders (SDS–SWCNTs) available during adsorption and the inherent attractive interaction between SWCNTs make cooperative adsorption likely. Although assuming Langmuir behavior can provide some insight into the thermodynamics of the separation process, great care must be taken when attempting to extract specific adsorption parameters by use of the relatively simple Langmuir model in complex systems. The complex nature of the isotherms observed in this study indicates that more detailed calorimetric studies are needed to

determine the thermodynamics of solute coverage, which is beyond the scope of this study.

## CONCLUSIONS

The development of a simple, large-scale process to separate SWCNTs is still needed, and consequently, the selective adsorption of SWCNTs onto agarose remains a promising method. Fully understanding the mechanism of selective adsorption should lead to more effective separations. In this study, we systematically altered the backbone of agarose to vary the relative importance of ionic, hydrophobic, and  $\pi$ – $\pi$  interactions during the adsorption between agarose and SWCNTs suspended with SDS. The results demonstrated that any alterations to agarose significantly reduced retention and selectivity. This inverse behavior and the inherent charge neutrality of agarose indicate that the large permanent dipole moments exhibited by agarose are critical to the adsorption process. Combined with the importance of the electrical double layer on nanotubes, it is proposed that ion–dipole interactions between the anionic charges on SDS–SWCNTs and the permanent dipoles of agarose are the dominant interaction in the adsorption process. The dissimilarities in polarizability of m- and s-SWCNTs result in different magnitudes of image charges on the nanotubes, thus altering the packing of surfactant on the sidewall. These different structures also limit the mobility of the surfactant. However, adsorption based solely on enthalpic effects cannot account for the dissimilar behavior of SWCNTs suspended in SDS and other surfactants, such as SC. Therefore, selectivity is considered to be driven by both enthalpic and entropic effects. Finally, the non-Langmuir isotherms observed during equilibrium studies indicates that great care must be taken when attempting to extract thermodynamic information without the additional data provided by calorimetric studies.

## ASSOCIATED CONTENT

### Supporting Information

Additional text and six figures showing characterization of SWCNT suspensions; adsorption isotherms, elution curves, and absorbance spectra for all gels used in nonequilibrium studies; and expanded details on mass fraction calculations. This material is available free of charge via the Internet at <http://pubs.acs.org>.

## AUTHOR INFORMATION

### Corresponding Author

kziegler@che.ufl.edu

### Present Addresses

<sup>§</sup>(C.A.S.B.) Materials Science and Engineering Division, National Institute of Standards and Technology, Gaithersburg, MD 20899

<sup>||</sup>(S.Y.) Environmental Resource Management, Jun-Gu Seoul, Korea 100-859.

### Notes

The authors declare no competing financial interest.

## ACKNOWLEDGMENTS

We acknowledge the National Science Foundation (CBET-0853347) for support of this research. C.A.S.B. thanks SEAGEP at the University of Florida for their support. We are grateful to Professor Yiider Tseng for access to the ultracentrifuge, the Richard Smalley Institute at Rice University for supplying

749 SWCNTs, and GE Health Care for providing Sepharose 6 and  
750 4 FF used in this study.

## 751 ■ REFERENCES

- 752 (1) De Volder, M. F. L.; Tawfick, S. H.; Baughman, R. H.; Hart, A. J.  
753 *Science* **2013**, 339, 535–539.
- 754 (2) Wilder, J. W. G.; Venema, L. C.; Rinzler, A. G.; Smalley, R. E.;  
755 Dekker, C. *Nature* **1998**, 391, 59–62.
- 756 (3) Komatsu, N.; Wang, F. *Materials* **2010**, 3, 3818–3844.
- 757 (4) Wang, H.; Ren, F.; Liu, C.; Si, R.; Yu, D.; Pfeifferle, L. D.; Haller,  
758 G. L.; Chen, Y. J. *Catal.* **2013**, 300, 91–101.
- 759 (5) Shi, D.; Resasco, D. E. *Chem. Phys. Lett.* **2011**, 511, 356–362.
- 760 (6) Hersam, M. C. *Nat. Nanotechnol.* **2008**, 3, 387–394.
- 761 (7) Liu, J.; Hersam, M. C. *MRS Bull.* **2010**, 35, 315–321.
- 762 (8) Arnold, M. S.; Green, A. A.; Hulvat, J. F.; Stupp, S. I.; Hersam, M.  
763 C. *Nat. Nanotechnol.* **2006**, 1, 60–65.
- 764 (9) Niyogi, S.; Densmore, C. G.; Doorn, S. K. *J. Am. Chem. Soc.* **2009**,  
765 131, 1144–1153.
- 766 (10) Tanaka, T.; Jin, H.; Miyata, Y.; Kataura, H. *Appl. Phys. Express*  
767 **2008**, 1, No. 114001.
- 768 (11) Mesgari, S.; Poon, Y. F.; Yan, L. Y.; Chen, Y.; Loo, L. S.; Thong,  
769 Y. X.; Chan-Park, M. B. *J. Phys. Chem. C* **2012**, 116, 10266–10273.
- 770 (12) Lu, J.; Lai, L.; Luo, G.; Zhou, J.; Qin, R.; Wang, D.; Wang, L.;  
771 Mei, W. N.; Li, G.; Gao, Z.; Nagase, S.; Maeda, Y.; Akasaka, T.; Yu, D.  
772 *Small* **2007**, 3, 1566–1576.
- 773 (13) Miyata, Y.; Maniwa, Y.; Kataura, H. *J. Phys. Chem. B* **2006**, 110,  
774 25–29.
- 775 (14) Tu, X.; Manohar, S.; Jagota, A.; Zheng, M. *Nature* **2009**, 460,  
776 250–253.
- 777 (15) Zheng, M.; Jagota, A.; Semke, E.; Diner, B.; Mclean, R.; Lustig,  
778 S.; Richardson, R.; Tassi, N. *Nat. Mater.* **2003**, 2, 338–342.
- 779 (16) Nish, A.; Hwang, J.; Doig, J.; Nicholas, R. *Nat. Nanotechnol.*  
780 **2007**, 2, 640–646.
- 781 (17) Dalton, A. B.; Stephan, C.; Coleman, J. N.; McCarthy, B.;  
782 Ajayan, P. M.; Lefrant, S.; Bernier, P.; Blau, W. J.; Byrne, H. J. *J. Phys.*  
783 *Chem. B* **2000**, 104, 10012–10016.
- 784 (18) Khripin, C. Y.; Fagan, J. A.; Zheng, M. *J. Am. Chem. Soc.* **2013**,  
785 135, 6822–6825.
- 786 (19) Chattopadhyay, D.; Galeska, I.; Papadimitrakopoulos, F. J. *Am.*  
787 *Chem. Soc.* **2003**, 125, 3370–3375.
- 788 (20) Ju, S.-Y.; Utz, M.; Papadimitrakopoulos, F. J. *Am. Chem. Soc.*  
789 **2009**, 131, 6775–6784.
- 790 (21) Liu, H.; Feng, Y.; Tanaka, T.; Urabe, Y.; Kataura, H. *J. Phys.*  
791 *Chem. C* **2010**, 114, 9270–9276.
- 792 (22) Tanaka, T.; Urabe, Y.; Nishide, D.; Kataura, H. *Appl. Phys.*  
793 *Express* **2009**, 2, No. 125002.
- 794 (23) Silvera-Batista, C. A.; Scott, D. C.; McLeod, S. M.; Ziegler, K. J.  
795 *J. Phys. Chem. C* **2011**, 115, 9361–9369.
- 796 (24) Tvrdy, K.; Jain, R. M.; Han, R.; Hilmer, A. J.; McNicholas, T. P.;  
797 Strano, M. S. *ACS Nano* **2013**, 7, 1779–1789.
- 798 (25) Xu, Z.; Yang, X.; Yang, Z. *Nano Lett.* **2010**, 10, 985–991.
- 799 (26) Tummala, N.; Striolo, A. *ACS Nano* **2009**, 3, 595–602.
- 800 (27) Hagel, L.; Ostberg, M.; Andersson, T. *J. Chromatogr. A* **1996**,  
801 743, 33–42.
- 802 (28) DePhillips, P.; Lenhoff, A. M. *J. Chromatogr. A* **2000**, 883, 39–  
803 54.
- 804 (29) Yao, Y.; Lenhoff, A. M. *J. Chromatogr. A* **2006**, 1126, 107–119.
- 805 (30) Evans, D. R.; Macniven, R. P.; Labanca, M.; Walker, J.;  
806 Notarnicola, S. M. *J. Chromatogr. A* **2008**, 1177, 265–271.
- 807 (31) Moore, V. C.; Strano, M. S.; Haroz, E. H.; Hauge, R. H.;  
808 Smalley, R. E.; Schmidt, J.; Talmon, Y. *Nano Lett.* **2003**, 3, 1379–1382.
- 809 (32) Khripin, C. Y.; Tu, X.; Heddleston, J. M.; Silvera-Batista, C.;  
810 Hight Walker, A. R.; Fagan, J.; Zheng, M. *Anal. Chem.* **2013**, 85,  
811 1382–1388.
- 812 (33) Tako, M.; Nakamura, S. *Carbohydr. Res.* **1988**, 180, 277–284.
- 813 (34) Arnott, S.; Fulmer, A.; Scott, W. E.; Dea, I. C. M.; Moorhouse,  
814 R.; Rees, D. A. *J. Mol. Biol.* **1974**, 9, 269–284.
- 815 (35) Stellwagen, J.; Stellwagen, N. C. *Biopolymers* **1994**, 34, 187–201.
- (36) Stellwagen, J.; Stellwagen, N. C. *Biopolymers* **1994**, 34, 1259–  
1273. 816
- (37) Stellwagen, J.; Stellwagen, N. C. *Nucleic Acids Res.* **1989**, 17,  
1537–1548. 817
- (38) Dormoy, Y.; Candau, S. *Biopolymers* **1991**, 31, 109–117. 818
- (39) Dubin, P., Ed. *Aqueous Size-Exclusion Chromatography*; Elsevier:  
Amsterdam, 1988. 819
- (40) Scopes, R. K. *Protein Purification: Principles and Practice*, 3rd ed.;  
Springer-Verlag: New York, 1994. 820
- (41) Stellan, H.; Jerten, J. R.; Pahlman, S. *J. Chromatogr.* **1974**, 101,  
281–288. 821
- (42) Liu, H.; Nishide, D.; Tanaka, T.; Kataura, H. *Nat. Commun.* **2011**,  
2, 309. 822
- (43) Tanaka, T.; Jin, H.; Miyata, Y.; Fujii, S.; Suga, H.; Naitoh, Y.;  
Minari, T.; Miyadera, T.; Tsukagoshi, K.; Kataura, H. *Nano Lett.* **2009**,  
9, 1497–1500. 823
- (44) Hirano, A.; Tanaka, T.; Kataura, H. *J. Phys. Chem. C* **2011**, 115,  
21723–21729. 824
- (45) Schaeffel, D.; Yordanov, S.; Schmelzeisen, M.; Yamamoto, T.;  
Kappl, M.; Schmitz, R.; Dunweg, B.; Butt, H.-J.; Koynov, K. *Phys. Rev.*  
*E* **2013**, 87, No. 051001R. 825
- (46) Duque, J. G.; Densmore, C. G.; Doorn, S. K. *J. Am. Chem. Soc.* **2010**,  
132, 16165–16175. 826
- (47) Silvera-Batista, C. A.; Weinberg, P.; Butler, J. E.; Ziegler, K. J. *J.*  
*Am. Chem. Soc.* **2009**, 131, 12721–12728. 827
- (48) Wang, R. K.; Chen, W.-C.; Campos, D. K.; Ziegler, K. J. *J. Am.*  
*Chem. Soc.* **2008**, 130, 16330–16337. 828
- (49) Rajter, R. F.; Podgornik, R.; Parsegian, V. A.; French, R. H.;  
Ching, W. Y. *Phys. Rev. B* **2007**, 76, No. 045417. 829
- (50) Hobbie, E. K.; Ihle, T.; Harris, J. M.; Semler, M. R. *Phys. Rev. B* **2012**,  
85, No. 245439. 830
- (51) Niyogi, S.; Boukhalfa, S.; Chikkannanavar, S. B.; McDonald, T. **2007**,  
129, 1898–1899. 831
- (52) Chen, R. J.; Zhang, Y.; Wang, D.; Dai, H. *J. Am. Chem. Soc.* **2001**,  
123, 3838–3839. 832
- (53) Tan, T.; Su, Z.-G.; Gu, M.; Xu, J.; Janson, J.-C. *Biotechnol. J.* **2010**,  
5, 505–510. 833
- (54) Lustig, S. R.; Jagota, A.; Khripin, C.; Zheng, M. *J. Phys. Chem. B* **2005**,  
109, 2559–2566. 834
- (55) Kozinsky, B.; Marzari, N. *Phys. Rev. Lett.* **2006**, 96, No. 166801. 835
- (56) Lu, W.; Xiong, Y.; Hassani, A.; Zhao, W.; Zheng, M.; Chen, L. *Nano*  
*Lett.* **2009**, 9, 1668–1672. 836
- (57) Silvera-Batista, C. A.; Ziegler, K. J. *Langmuir* **2011**, 27, 11372–  
11380. 837
- (58) Israelachvili, J. N. *Intermolecular and Surface Forces*, 2nd ed.;  
Academic Press: San Diego, CA, 1991. 838
- (59) Chandler, D. *Nature* **2002**, 417, 491–491. 839
- (60) Inori, R.; Okada, T.; Arie, T.; Akita, S. *Nanotechnology* **2012**, 23,  
7. 840
- (61) Lukaszczuk, P.; Rummeli, M. H.; Knupfer, M.; Kalenczuk, R. J.;  
Borowiak-Palen, E. *Mater. Res. Bull.* **2012**, 47, 687–691. 841
- (62) Foo, K. Y.; Hameed, B. H. *Chem. Eng. J.* **2010**, 156, 2–10. 842
- (63) Hirano, A.; Tanaka, T.; Urabe, Y.; Kataura, H. *J. Phys. Chem. C* **2012**,  
116, 9816–9823. 843
- (64) Hirano, A.; Tanaka, T.; Kataura, H. *ACS Nano* **2012**, 6, 10195–  
10205. 844
- (65) Giles, C. H.; Smith, D. J. *Colloid Interface Sci.* **1974**, 47, 755–  
765. 845